Robust Adaptive Neural Network-Based Backstepping Tracking for Second-Order Euler-Lagrange Systems with Unknown Parameters

Shen Zhang[1,2], Xiaozheng Jin[1,2*], and Na Li[3]

[1] Key Laboratory of Computing Power Network and Information Security, Ministry of Education, Shandong Computer Science Center (National Supercomputer Center in Jinan), Qilu University of Technology (Shandong Academy of Sciences), Jinan 250353, China
[2] Shandong Provincial Key Laboratory of Industrial Network and Information System Security, Shandong Fundamental Research Center for Computer Science, Jinan 250013, China
[3] School of Intelligent Manufacturing and Control Engineering, Qilu Institute of Technology, Jinan 250200, Shandong, China

*Corresponding author: xzjin@qlu.edu.cn

Abstract. A robust adaptive tracking control approach is designed for second-order Euler–Lagrange systems operating under dynamic uncertainties, parameter perturbations, and external disturbances. Instead of relying on precise nominal model information, the unknown effects are collected into a lumped perturbation term. To deal with the state-dependent nonlinear bounding function, an RBF neural network is employed for approximation. Meanwhile, several adaptive laws are constructed to adjust the unknown constants linked to the input and disturbance terms. The controller is constructed through a backstepping procedure and further equipped with a sigma-modification mechanism, so that discontinuous robust compensation can be avoided. The Lyapunov-based stability proof demonstrates that the closed-loop system maintains uniform ultimate boundedness of all signals, while the tracking errors are driven into a small residual set. Simulation results on an underactuated unmanned surface vehicle demonstrate accurate tracking performance, bounded adaptive parameters, and smooth control inputs.
Keywords: Euler-Lagrange Systems, Robust Adaptive Control, RBF Neural Networks, Backstepping, Chattering Attenuation

1 Introduction

Euler-Lagrange (EL) models are widely used to describe second-order nonlinear electromechanical systems, such as robotic manipulators, humanoid robots, aerospace platforms, and marine vehicles [1-3]. Among them, unmanned surface vehicles (USVs) have received increasing attention due to their potential applications in ocean observation, environmental monitoring, maritime rescue, and autonomous navigation [4,5]. However, high-accuracy trajectory tracking for USVs remains challenging because their dynamics involve strong nonlinear coupling, underactuation, parameter variations, and unknown external disturbances [6-8]. In practical scenarios, the surge, sway, and yaw motions are coupled by hydrodynamic effects, while the available actuators cannot directly regulate all degrees of freedom [9]. In addition, inertia and hydrodynamic coefficients are difficult to identify accurately and may vary under different operating conditions [10,11]. Wind, waves, and currents further introduce time-varying perturbations, which may degrade the closed-loop tracking performance [12,13].

For EL systems and marine vehicles, numerous control schemes have been reported in existing studies. Among them, conventional model-based controllers, such as computed-torque and PID methods, are easy to implement, but satisfactory performance generally requires an accurate system model [14]. Sliding-mode control can enhance robustness against matched uncertainties through switching actions [15,16], but the resulting chattering may excite unmodeled dynamics and increase actuator wear [17-19]. Although boundary-layer and smoothing techniques can reduce chattering, they often sacrifice part of the tracking accuracy [20]. Adaptive backstepping provides a recursive design framework for strict-feedback nonlinear systems [21,22], whereas many existing adaptive methods still require linear parameterization or known bounds of uncertain terms, which limits their applicability to complex USV dynamics [23, 24].

To reduce the dependence on accurate model information, neural networks and fuzzy approximators have been incorporated into adaptive control designs. RBF neural networks are especially attractive because of their simple structure, local approximation ability, and convenient online update form. They have been combined with backstepping controllers to handle nonlinear uncertainties in EL systems [25-27]. Nevertheless, many existing neural adaptive approaches still require partial prior knowledge, such as known inertia bounds or bounded approximation structures [28]. Some methods also introduce sign-type robust terms [29], which may produce nonsmoothed control signals. Accordingly, developing a smooth adaptive tracking control scheme capable of simultaneously addressing model uncertainties and external disturbances remains of practical significance.

To handle parametric uncertainties and external perturbations in second-order EL systems, this study designs a neural-network-assisted robust adaptive backstepping controller. The primary contributions of this paper are highlighted in the following aspects. 1) The proposed controller does not rely on accurate nominal model information. Instead, the state-dependent nonlinear bounding function is approximated through an RBF neural-network-based estimator. while the residual unknown constants are updated through online adaptive mechanisms. 2) A sigma-modification technique is embedded in both the controller design and the adaptive update rules, which can prevent over-adjustment of adaptive parameters and contribute to smoother control signals. 3) A Lyapunov stability proof is established to demonstrate that the boundedness of the closed-loop system can be guaranteed, while the tracking errors eventually approach a small neighborhood near the equilibrium point. 4) Numerical simulations on an underactuated USV are conducted to evaluate the proposed scheme in terms of trajectory-tracking performance, robustness, and chattering attenuation.

The subsequent sections are organized as follows. In Section II, the EL system model is established, and the tracking control problem is formulated. Section III is devoted to the design of the proposed controller and the Lyapunov-based stability proof. Section IV demonstrates simulation studies on the USV system. The main conclusions are drawn in Section V.

2 Problem Formulation

2.1 System Formulation

The second-order Euler-Lagrange system is described by the following dynamic equation:

$$D(p)\ddot{p} + V(p,\dot{p})\dot{p} + G(p) + d = \tau, \tag{1}$$

where $p(t) \in \mathbb{R}^n$ and $\dot{p}(t) \in \mathbb{R}^n$ stand for the generalized position and velocity vectors, respectively. Moreover, $D(p) \in \mathbb{R}^{n\times n}$ is a symmetric positive definite inertia matrix, $V(p,\dot{p}) \in \mathbb{R}^{n\times n}$ represents the Coriolis and centrifugal matrix, and $G(p) \in \mathbb{R}^n$ is the gravitational vector. The term $\tau \in \mathbb{R}^n$ denotes the control input, while $d \in \mathbb{R}^n$ represents external disturbances with bounded norms.

By introducing the velocity state vector $\dot{p}(t) = v(t)$, by defining the corresponding state variables, (1) is transformed into the following state-space model:

$$\begin{cases} \dot{p} = v, \\ \dot{v} = D(p)^{-1}\tau - D(p)^{-1}\big(V(p,\dot{p})v + G(p)\big) + D(p)^{-1}d, \end{cases} \tag{2}$$

In practical operating conditions, the actual system parameters may deviate from their nominal values due to modeling errors, parameter variations, and environmental effects.

Let $D(p) = D_0(p) + \Delta D(p)$, $V(p,v) = V_0(p,v) + \Delta V(p,v)$, and $G(p) = G_0(p) + \Delta G(p)$, where $\{D_0, V_0, G_0\}$ are defined as the nominal but unknown terms corresponding to inertia, Coriolis/centripetal effects, and gravity, respectively, while $\{\Delta D, \Delta V, \Delta G\}$ denote the corresponding unknown uncertainties. For simple formulation, the dynamic (2) can be expressed by

$$\begin{cases} \dot{p} = v \\ \dot{v} = \big(D_0(p) + \Delta D\big)^{-1}\tau \\ \qquad - \big(D_0(p) + \Delta D\big)^{-1}\big[\big(V_0(p,\dot{p}) + \Delta V\big)v + G_0(p) + \Delta G\big] \\ \qquad + \big(D_0(p) + \Delta D\big)^{-1}d \end{cases} \tag{3}$$

Furthermore, we can obtain

$$\begin{cases} \dot{p} = v \\ \dot{v} = D_0^{-1}\tau - D_0^{-1}V_0 v + W_d \end{cases} \tag{4}$$

where $W_d = - D_0^{-1}(\Delta V v + \Delta G) - E_D(Vv + G) + E_D\tau + E_D d, E_D = D^{-1} - D_0^{-1}$.

For simple statement, we define that

$$C_1 = D_0^{-1}V_0, C_2 = D_0^{-1} \tag{5}$$

which leads to

$$\begin{cases} \dot{p} = v \\ \dot{v} = C_2\tau - C_1 v + W_d \end{cases} \tag{6}$$

Based on (4) the following condition for perturbations $|W_d(t)| \in \mathbb{R}$ is assumed to be satisfied by:

Assumption 1. The lumped perturbation $W_d(t)$ is assumed to satisfy an admissible upper bound composed of state-dependent and input-dependent components.

$$|W_d| \leqslant \lambda_\tau|\tau| + \vartheta(p,v) + \overline{\lambda}_d \tag{7}$$

where λ_τ and $\overline{\lambda}_d$ are unknown positive constants. $\vartheta(p,v)$ denotes an unknown, continuous, and positive nonlinear function depending on the system states p and v.

Remark 1. This assumption allows the perturbation term $W_d(t)$ to vary with the system states p, v and τ. Therefore, it can cover unmodeled friction, non-conservative forces, hydrodynamic uncertainty, and external disturbances. Compared with fixed norm-bounded assumptions in (7), this form is more flexible for describing nonlinear EL-system uncertainties.

2.2 Control Objective

Let the desired trajectory $p_d(t) \in \mathbb{R}^n$ be smooth and have bounded derivatives. The tracking error of the position variable is introduced as follows:

$$z_1(t) = p(t) - p_d(t) \tag{8}$$

This work focuses on designing a robust adaptive neural-network-based control input $\tau(t)$ to guarantee that the position state $p(t)$ can follow the reference signal $p_d(t)$ despite the disturbance $W_d(t)$ and the absence of prior knowledge of system parameters, subject to the following condition:

$$\lim_{t\to\infty}|z_1(t)| \leq \varrho \tag{9}$$

where ϱ is a small residual bound proportional to σ.

2.3 RBF Neural Networks

Motivated by Assumption1, an RBFNN-based approximation is introduced to characterize the unknown nonlinear mapping $\vartheta(p,v)$ involved in (4). By choosing $Z=[p^T,v^T]^T$ as the input of the network, the following approximation form is adopted:

$$\vartheta(p,v)=W^T h(Z)+\epsilon(Z),$$

where $W\in\mathbb{R}^q$ is the ideal but unknown weight vector and $q>1$ denotes the number of radial basis neurons. The term $\epsilon(Z)$ accounts for the approximation mismatch and satisfies $|\epsilon(Z)|\leq\overline{\epsilon}$, where $\overline{\epsilon}>0$ is an unknown upper bound.

The vector $h(Z)=[h_1(Z),\dots,h_q(Z)]^T$ consists of Gaussian basis functions, which are defined by

$$h_l(Z)=\exp\left[-\frac{(Z-d_{il})^T(Z-d_{il})}{g_l^2}\right],\quad l=1,2,\dots,q, \tag{10}$$

in which d_{il} is defined as the center associated with the l-th hidden neuron, while g_l is a positive parameter determining its width.

3 Robust Adaptive Control Synthesis for Uncertain Second-Order Euler-Lagrange Systems

The controller is derived from a backstepping procedure under the Lyapunov framework. At each design step, an appropriate Lyapunov function is constructed, and the corresponding stabilizing signal is selected. Adaptive compensation terms are then introduced to handle the unknown constants and nonlinear perturbations. In this way, robust tracking can be achieved without requiring the exact matrices of the EL system.

Step1. Using the error variable introduced in (8), the corresponding first error subsystem is expressed as:

$$\dot{z}_1=v(t)-p_d(t) \tag{11}$$

where $\dot{p}=v$ according to (6).

In order to establish the stability of the first error subsystem described by (11), the following positive definite Lyapunov candidate is adopted:

$$V_1(t)=\frac{1}{2}z_1^T z_1$$

and its derivative becomes

$$\dot{V}_1(t)=-z_1^T K_1 z_1+z_1^T\left(K_1 z_1+v-\dot{p}_d\right) \tag{12}$$

where $K_1>0$ is a positive definite gain matrix. It follows that $\dot{V}_1<0$ whenever $z_1(t)\neq 0$, which ensures the asymptotic convergence of $z_1(t)$ to zero.

To render $\dot{V}_1(t)=-z_1^T K_1 z_1$, a virtual control signal is introduced based on (12) as:

$$\alpha=-K_1 z_1+\dot{p}_d \tag{13}$$

If v converges to α as $t\to\infty$, then $\dot{V}_1(t)=-z_1^T K_1 z_1<0$ holds, and by Barbital's lemma, $\lim_{t\to\infty}|z_1(t)|=0$ is guaranteed. Accordingly, the next step aims to drive $\lim_{t\to\infty}\left(v(t)-\alpha(t)\right)=0$.

Step2. Define the second error variable by comparing the actual velocity state with the virtual control signal:

$$z_2=v(t)-\alpha(t) \tag{14}$$

It can be implied from (12) and (13) we yield

$$\dot{z}_2=-K_1^T K_1 z_1+K_1 z_2-\ddot{p}_d-C_1 v+C_2\tau+W_d \tag{15}$$

Since the exact model matrices D,V and G are unavailable, to deal with the lumped uncertain term, the following adaptive robust compensation law is introduced:

$$\begin{aligned}\tau(t)&=\hat{C}_2^{-1}\left(-z_1+\Omega+\hat{C}_1 v-K_2 z_2+\Psi\right)\\ \Psi&=-\frac{z_2}{|z_2|+\sigma}\left(\hat{\lambda}_\tau|\tau|+\hat{W}^T h(v)+\hat{\lambda}_d\right)\end{aligned} \tag{16}$$

The corresponding update laws for the unknown parameters and neural-network weights are selected as follows:

$$\frac{d\dot{\hat{C}}_1}{dt} = \begin{cases} -\Gamma_{C_1} z_2 v^T, & |z_2| > \sigma \\ 0, & |z_2| \le \sigma \end{cases} \tag{17}$$

$$\frac{d\dot{\hat{C}}_2}{dt} = \begin{cases} \Gamma_{C_2} z_2 \tau^T, & |z_2| > \sigma \\ 0, & |z_2| \le \sigma \end{cases} \tag{18}$$

$$\frac{d\dot{\hat{W}}(t)}{dt} = \begin{cases} \Gamma_W h(Z)|z_2|, & |z_2| > \sigma \\ 0, & |z_2| \le \sigma \end{cases} \tag{19}$$

$$\frac{d\dot{\hat{\lambda}}_\tau}{dt} = \begin{cases} \gamma_\tau |z_2||\tau|, & |z_2| > \sigma \\ 0, & |z_2| \le \sigma \end{cases} \tag{20}$$

$$\frac{d\dot{\hat{\lambda}}_d}{dt} = \begin{cases} \gamma_d |z_2|, & |z_2| > \sigma \\ 0, & |z_2| \le \sigma \end{cases} \tag{21}$$

where $\sigma > 0$ is a small design constant, $\Omega = - K_1 z_2 + K_1^T K_1 z_1 + \ddot{p}_d$. The quantities $\hat{C}_1, \hat{C}_2, \hat{\lambda}_\tau, \hat{\lambda}_d$, and $\hat{W}$ denote the online estimates of the unknown constants $C_1, C_2, \lambda_\tau, \lambda_d$, and the neural network weight vector W, respectively, all of which are updated via the adaptive laws given in (17)-(21). The matrices Γ_{C_1}, Γ_{C_2}, and Γ_w are symmetric positive-definite learning rate matrices, while $\gamma_\tau > 0$ and $\gamma_d > 0$ are scalar adaptation gains.

Let

$$\tilde{C}_1(t) = \hat{C}_1(t) - C_1, \quad \tilde{C}_2(t) = \hat{C}_2(t) - C_2,$$
$$\tilde{\lambda}_\tau(t) = \hat{\lambda}_\tau(t) - \lambda_\tau, \quad \tilde{\lambda}_d(t) = \hat{\lambda}_d(t) - \lambda_d.$$

And $\tilde{W} = \hat{W}(t) - W$. Since $C_1, C_2, \lambda_\tau, \lambda_d$ and W are constant, the following adaptive error systems can be obtained by:

$$\begin{aligned} &\frac{d\tilde{C}_1(t)}{dt} = \frac{d\hat{C}_1(t)}{dt}, \quad \frac{d\tilde{C}_2(t)}{dt} = \frac{d\hat{C}_2(t)}{dt}, \\ &\frac{d\tilde{\lambda}_\tau(t)}{dt} = \frac{d\hat{\lambda}_\tau(t)}{dt}, \quad \frac{d\tilde{\lambda}_d(t)}{dt} = \frac{d\hat{\lambda}_d(t)}{dt}, \\ &\frac{d\tilde{W}(t)}{dt} = \frac{d\hat{W}(t)}{dt}. \end{aligned} \tag{22}$$

For the second-order Euler–Lagrange system (6) with fully unavailable system matrices D , V , and G , the stability of the resulting closed-loop system and the corresponding tracking performance under the proposed controller are established in the theorem below.

Theorem 1 Consider system (6) under the perturbation condition given in Assumption 1. Under the implementation of the developed robust adaptive neural-network tracking control law $\tau(t)$ and the associated adaptation mechanisms for $\hat{C}_1$, $\hat{C}_2$, $\hat{W}$, $\hat{\lambda}_\tau$, and $\hat{\lambda}_d$, the proposed controller ensures bounded behavior of the closed-loop system, meaning that all involved signals are kept within finite bounds. In addition, the two error states are finally driven into a small residual set containing the origin, namely

$$\lim_{t\to\infty}|z_1(t)|\leq\varrho,\text{and}\lim_{t\to\infty}|z_2(t)|\leq\varrho,$$

where ϱ is determined by the σ-modification term and can be made small through proper parameter selection.

Proof. The following Lyapunov candidate is selected to include the tracking errors, the estimation errors of adaptive parameters, and the neural-network weight estimation error:

$$\begin{aligned}V=&\frac{1}{2}z_1^Tz_1+\frac{1}{2}z_2^Tz_2+\frac{1}{2}\mathrm{tr}\left(\tilde{C}_1^T\Gamma_{C_1}^{-1}\tilde{C}_1\right)+\frac{1}{2}\mathrm{tr}\left(\tilde{C}_2^T\Gamma_{C_2}^{-1}\tilde{C}_2\right)\\&+\frac{1}{2}\mathrm{tr}\left(\tilde{W}^T\Gamma_w^{-1}\tilde{W}\right)+\frac{1}{2\lambda_\tau}\tilde{\lambda}_\tau^2+\frac{1}{2\lambda_d}\tilde{\lambda}_d^2\end{aligned}\tag{23}$$

Substituting the control law τ in (16) and the adaptive laws (17)-(21) into (23), and considering the region where $|z_2|>\sigma$, the time derivative of V satisfies

$$\begin{aligned}\dot{V}\leqslant&-z_1^TK_1z_1-z_2^TK_2z_2+z_2^T\tilde{C}_1v-z_2^T\tilde{C}_2\tau+z_2^T\Psi\\&+z_2^TW_d+\frac{1}{2}\mathrm{tr}\left(\tilde{C}_1^T\Gamma_{C_1}^{-1}\tilde{C}_1\right)+\frac{1}{2}\mathrm{tr}\left(\tilde{C}_2^T\Gamma_{C_2}^{-1}\tilde{C}_2\right)\\&+\frac{1}{2}\mathrm{tr}\left(\tilde{W}^T\Gamma_W^{-1}\tilde{W}\right)+\frac{1}{2\lambda_\tau}\tilde{\lambda}_\tau^2+\frac{1}{2\lambda_d}\tilde{\lambda}_d^2\\\leqslant&-z_1^TK_1z_1-z_2^TK_2z_2+z_2^T\tilde{C}_1v-z_2^T\tilde{C}_2\tau\\&-\frac{|z_2|^2}{|z_2|+\sigma}\left(\hat{\lambda}_\tau|\tau|+\hat{W}^Th(Z)+\hat{\lambda}_d\right)\\&+|z_2|(\lambda_\tau|\tau|+W^Th(Z)+\lambda_d)+\frac{1}{2}\mathrm{tr}\left(\tilde{C}_1^T\Gamma_{C_1}^{-1}\tilde{C}_1\right)\\&+\frac{1}{2}\mathrm{tr}\left(\tilde{C}_2^T\Gamma_{C_2}^{-1}\tilde{C}_2\right)+\frac{1}{2}\mathrm{tr}\left(\tilde{W}^T\Gamma_W^{-1}\tilde{W}\right)+\frac{1}{2\lambda_\tau}\tilde{\lambda}_\tau^2+\frac{1}{2\lambda_d}\tilde{\lambda}_d^2\end{aligned}\tag{24}$$

Then, we can obtain

$$\begin{aligned}\dot{V} \leqslant & - z_1^T K_1 z_1 - z_2^T K_2 z_2 + \frac{\sigma|z_2|\left(\hat{\lambda}_\tau|\tau| + \hat{W}^T h(Z) + \hat{\lambda}_d\right)}{|z_2| + \sigma} \\ & + \operatorname{tr}\left(\tilde{C}_1^T\left(z_2 v^T + \Gamma_{C_1}^{-1}\dot{\tilde{C}}_1\right)\right) + \operatorname{tr}\left(\tilde{C}_2^T\left(-z_2\tau^T + \Gamma_{C_2}^{-1}\dot{\tilde{C}}_2\right)\right) \\ & -|z_2|\tilde{\lambda}_\tau|\tau| - |z_2|\tilde{\lambda}_d + \operatorname{tr}\left(\tilde{W}^T\left(-h(Z)|z_2| + \Gamma_w^{-1}\dot{\tilde{W}}\right)\right) \\ & + \frac{1}{\gamma_\tau}\tilde{\lambda}_\tau\dot{\tilde{\lambda}}_\tau + \frac{1}{\gamma_d}\tilde{\lambda}_d\dot{\tilde{\lambda}}_d \\ \leqslant & - z_1^T K_1 z_1 - z_2^T K_2 z_2 + \sigma\left(\hat{\lambda}_\tau|\tau| + \hat{W}^T h(Z) + \hat{\lambda}_d\right)\end{aligned} \tag{25}$$

Furthermore,

$$\dot{V} \leq - \lambda_{\min}(K)|z|^2 + \Delta(\sigma), \tag{26}$$

where

$\lambda_{\min}(K) = \min\{\lambda_{\min}(K_1), \lambda_{\min}(K_2)\}$ and $\Delta(\sigma) = \sigma\left(\hat{\lambda}_\tau|\tau| + \hat{W}^T h(Z) + \hat{\lambda}_d\right)$.

Clearly, when $|z| > \sqrt{\Delta(\sigma)/\lambda_{\min}(K)}$, we have $\dot{V} < 0$. This implies that the error vector $z(t)$ will be eventually driven into the compact region defined as follows:

$$\Omega_z = \left\{z \in \mathbb{R}^{2n} \,|\, |z| \leq \sqrt{\frac{\Delta(\sigma)}{\lambda_{\min}(K)}}\right\}. \tag{27}$$

Consequently, the following conclusion can be drawn

$$\lim_{t\to\infty}|z_1(t)| \leq \varrho, \text{and} \lim_{t\to\infty}|z_2(t)| \leq \varrho, \tag{28}$$

where ϱ is a small constant proportional to σ.

4 A Simulation Example

Following the USV model in [30], a three-degree-of-freedom unmanned surface vehicle is employed as the simulation plant in this section. Its kinematic and dynamic equations are written as

$$\begin{cases}\dot{p} = J(\psi)v, \\ \dot{v} = M^{-1}\tau - M^{-1}((C(v) + D(v))v) + M^{-1}d\end{cases} \tag{29}$$

where $p:=(x,y,\psi)$ denotes the position and heading vector in the earth-fixed frame, and $v:=(v_x,v_y,v_\psi)$ represents the velocity vector expressed in the body-fixed frame. The inertia, Coriolis/centripetal, and damping matrices are supposed to contain nominal parts and uncertain perturbations, namely $M=M_0+\Delta M$, $C=C_0+\Delta C$, and

$D=D_0+\Delta D$. Here, M_0, C_0, and D_0 are the unknown nominal model matrices, while ΔM, ΔC, and ΔD describe the corresponding modeling errors and parameter variations. The vector d stands for unknown external disturbances, and τ is the control input. The kinematic transformation from the body-fixed frame to the earth-fixed frame is governed by the rotation matrix $J(\psi)$, defined as follows:

$$J(\psi)=\begin{bmatrix}\cos(\psi) & -\sin(\psi) & 0\\ \sin(\psi) & \cos(\psi) & 0\\ 0 & 0 & 1\end{bmatrix}.$$

Considering the practical operating environment, owing to modeling errors and variations in system parameters, the practical dynamic parameters of the USV generally cannot exactly match the nominal ones. Consequently, the dynamic model in (4) can be reformulated as

$$\begin{cases}\dot{p}=J(\psi)v\\ \dot{v}=M_0^{-1}\tau-M_0^{-1}\big(C_0(v)+D_0(v)\big)v+W_d\end{cases}$$

where

$$W_d=-M_0^{-1}(\Delta D+\Delta C)v-E_M(C+D)v+E_M\tau+M^{-1}d,$$
$$E_M=\big(M_0+\Delta M\big)^{-1}-M_0.$$

For notational brevity, define

$$C_1=M_0^{-1}\big(C_0+D_0\big),C_2=M_0^{-1}$$

which leads to

$$\begin{cases}\dot{p}=J(\psi)v\\ \dot{v}=C_2\tau-C_1v+W_d\end{cases}\tag{30}$$

In the simulations, M_0, C_0 and D_0 are the unknown and constant nominal matrices of inertia, Coriolis and centripetal and the hydrodynamic damping parameter. Parameter uncertainties are introduced as 20% deviations from the nominal values (i.e., $\Delta M=0.2M_0$, $\Delta C=0.2C_0$, $\Delta D=0.2D_0$). Additionally, time-varying external disturbances are injected into the system as

$d(t) = [0.5\sin(t), -0.1\cos(t), 0.1]^T$ to test the robustness. A circular path is adopted as the reference trajectory: $p_d(t) = \left[5\cos(0.2t), 5\sin(0.2t), 0.2t + \frac{\pi}{2}\right]^T$, with initial states aligned at $p(0) = \left[5, 0, \frac{\pi}{2}\right]^T$.

The parameters used in the control design are set to $K_1 = \mathrm{diag}[6]$ and $K_2 = \mathrm{diag}[27]$. The RBF neural network is constructed with 50 nodes, where the centers are randomly distributed in the space $[-10, 10] \times [-2, 2]$ and the width is set to 3.0. The adaptive learning rates are chosen as $\Gamma_W = 7.0I$, $[\Gamma_{C1}, \Gamma_{C2}] = 10^{-4}$, and $[\gamma_\tau, \gamma_d] = 10^{-3}$. A critical parameter for the proposed σ-modification mechanism is set to $\sigma = 0.35$ to eliminate chattering phenomenon.

The effectiveness of the proposed control strategy is demonstrated through the simulation results shown in Figs. 1-7. As depicted in Fig. 1, the USV can follow the given circular reference trajectory with good tracking precision. Figs. 2 and 3 respectively illustrate the temporal evolution of the position states x, y, ψ and the velocity states v_x, v_y, v_ψ. The actual trajectories are almost consistent with reference signals over the entire simulation interval.

The control signals, including the surge force and yaw moment, are plotted in Fig. 4. Their smooth profiles indicate that the proposed controller can avoid severe chattering while maintaining effective tracking performance. Figs. 5 and 6 further show the evolution of the adaptive estimates $\hat{C}_1$, $\hat{C}_2$, $\hat{\lambda}_\tau$, and $\hat{\lambda}_d$, all of which remain bounded and converge to stable ranges. Specifically, $\hat{\lambda}_\tau$ is used to handle the input-related uncertainty, whereas $\hat{\lambda}_d$ contributes to disturbance compensation. Finally, Fig. 7 presents the norm of the neural-network weight estimate $\hat{W}$, which verifies that the online learning parameters are well bounded.

5 Conclusion

In this study, a robust adaptive control method incorporating neural-network approximation and backstepping design was established for second-order Euler–Lagrange systems influenced by unknown parameters and external disturbances. By incorporating RBF neural-network approximation with adaptive backstepping and sigma-modified updating laws, the controller provides high tracking accuracy while avoiding nonsmooth control behavior. The Lyapunov-based proof shows that every signal generated by the closed-loop system remains within finite bounds, and the tracking errors are eventually restricted to a small residual set. The simulation results for an underactuated USV further demonstrate the effectiveness of the method in terms of robustness, tracking precision, and chattering reduction.

Future studies will consider the extension of this control framework to distributed multi-agent cooperative control and output-feedback scenarios where full-state measurements are not available.

Acknowledgments. Partial funding for this research was provided by the National Natural Science Foundation of China under Grant Nos. 62573247 and 62173193.

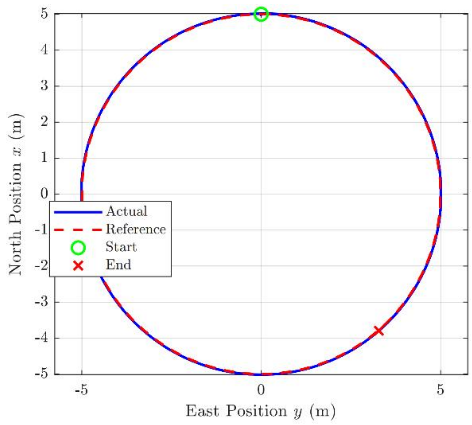

Fig. 1. Trajectory tracking performance of the USV.

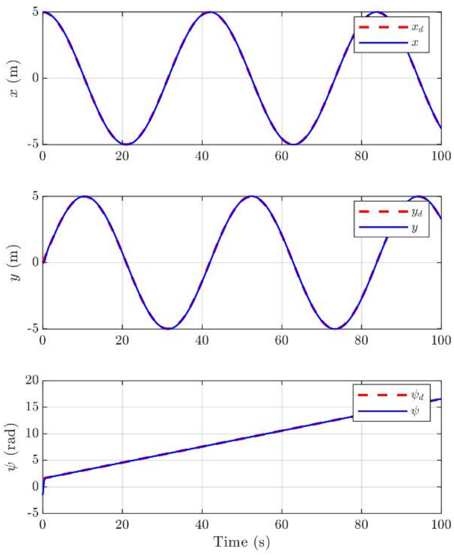

Fig. 2. Position responses and desired references of the USV.

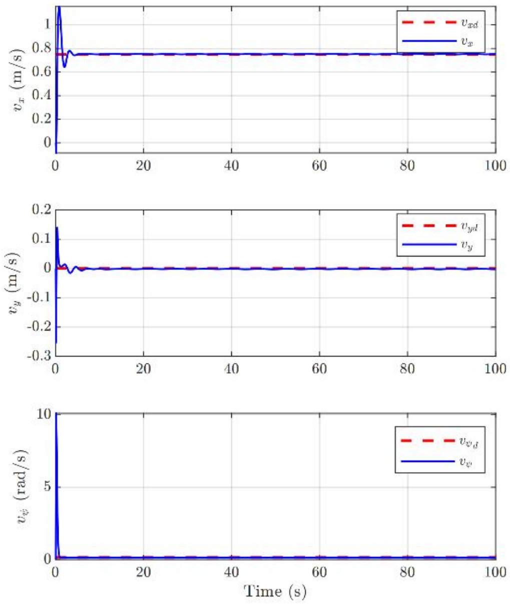

Fig. 3. Velocity responses and desired references of the USV.

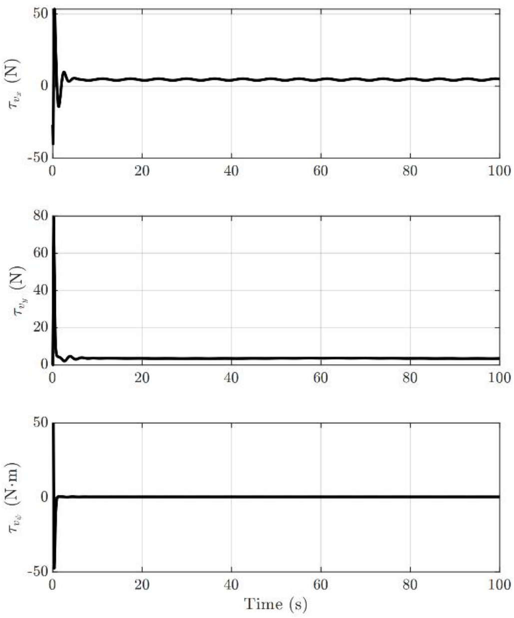

Fig. 4. Control input τ responses.

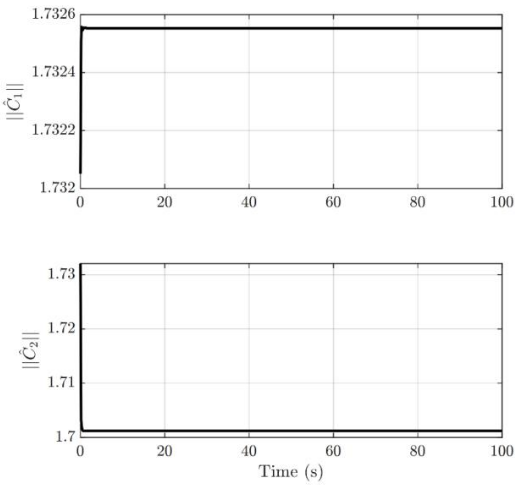

Fig. 5. Evolution curves of adaptive parameters $\hat{C}_1$ and $\hat{C}_2$.

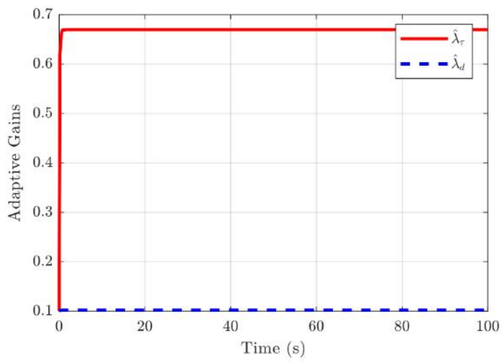

Fig. 6. Evolution curves of robust adaptive gains $\hat{\lambda}_\tau$ and $\hat{\lambda}_d$.

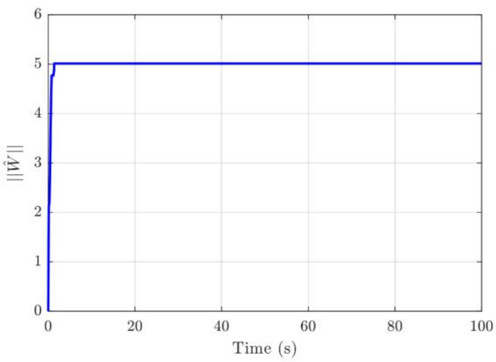

Fig. 7. Evolution of the neural-network weight norm.

References

1. R. Ortega, A. Loria, P. J. Nicklasson, and H. Sira-Ramirez, Passivity-based control of Euler-Lagrange systems: Mechanical, electrical and electromechanical applications. Springer London, 1998.
2. T. I. Fossen, Handbook of marine craft hydrodynamics and motion control. John Wiley & Sons, 2011.
3. X. Jin, J. Jiang, J. Qin, W. X. Zheng, and M. Gao, “Observer-based fixed-time-synchronized control for uncertain Euler-Lagrange systems with bias-actuator faults, IEEE Transactions on Cybernetics,” vol. 55, no. 8, 3811-3824, 2025.
4. Z. Liu, Y. Zhang, X. Yu, and C. Yuan, “Unmanned surface vehicles: An overview of developments and challenges,” Annual Reviews in Control, vol. 41, pp. 71–93, 2016.
5. S.-L. Dai, S. He, M. Wang, and C. Yuan, “Adaptive neural control of underactuated surface vessels with prescribed performance guarantees,” IEEE Transactions on Neural Networks and Learning Systems, vol. 30, no. 12, pp. 3686–3698, 2019.
6. X. Jin, C. Jiang, J. Qin, and W. X. Zheng, “Robust pinning constrained control and adaptive regulation of coupled Chua's circuit networks, IEEE Transactions on Circuits and Systems-I: Regular Papers,” vol. 66, no. 10, pp. 3928-3940, 2019.
7. H. Ye, S. Wu, W. Liu et al., “Adaptive neural synergetic heading control for USVs with unknown dynamics and disturbances,” Ocean Engineering, vol. 300, p. 117438, 2024.
8. X. Jin, J. Chi, J. Qin,W. X. Zheng, X. Wu, and W. Fu, “Robust security control of a class of second-order nonlinear systems against DoS attacks,” IEEE Transactions on Systems, Man and Cybernetics: Systems, vol. 56, no. 2, 1449-1463, 2026.
9. C. Barrera, I. Padron, F. S. Luis et al., “Trends and challenges in unmanned surface vehicles (USV): From survey to shipping,” TransNav: International Journal on Marine Navigation and Safety of Sea Transportation, vol. 15, no. 1, 2021.
10. Y. Dong and J. Chen, “Adaptive control for rendezvous problem of networked uncertain Euler–Lagrange systems,” IEEE Transactions on Cybernetics, vol. 49, no. 6, pp. 2190–2199, 2019.
11. J. Jiang, X. Jin, X. Xie, and H. Wang, “Nonlinear ELM estimator-based formation control for perturbed unmanned surface vehicle systems with prescribed performance,” IEEE Transactions on Intelligent Vehicles, vol. 9, no. 12, pp. 8175-8189, 2024.
12. Q. Yao, “Fixed-time trajectory tracking control for unmanned surface vessels in the presence of model uncertainties and external disturbances,” International Journal of Control, vol. 95, no. 5, pp. 1133–1143, 2022.
13. X.-Z. Jin, G.-H. Yang, and X.-H. Chang, “Robust H_∞ and adaptive tracking control against actuator faults with a linearised aircraft application,” International Journal of Systems Science, vol. 44, no. 1, pp. 151–165, 2013.
14. J. J. Craig, Introduction to robotics: mechanics and control, 3rd ed. Pearson Education India, 2009.
15. V. I. Utkin, “Sliding mode control design principles and applications to electric drives,” IEEE Transactions on Industrial Electronics, vol. 40, no. 1, pp. 23–36, 1993.
16. X.-Z. Jin, J. H. Park, “Adaptive sliding-mode insensitive control of a class of non-ideal complex networked systems,” Information Sciences, vol. 274, no. 1, pp. 273-285, 2014.
17. B. Li, Z. Ji, Z. Zhao et al., “Model predictive optimization and terminal sliding mode motion control for mobile robot with obstacle avoidance,” IEEE Transactions on Industrial Electronics, 2025.

18. M. Gao, L. Ding, X. Jin, “ELM-based adaptive faster fixed-time control of robotic manipulator systems,” IEEE Transactions on Neural Networks and Learning Systems, vol. 34, no. 8, pp. 4646-4658, 2023.
19. M. Gao, X. Jin, and L. Ding, “A novel nonsingular fixed-time sliding mode control of uncertain Euler-Lagrange systems,” IEEE Systems Journal, vol. 17, no. 1, pp. 467-478, 2023.
20. H. Dong, X. Yang, H. Gao et al., “Practical terminal sliding-mode control and its applications in servo systems,” IEEE Transactions on Industrial Electronics, vol. 70, no. 1, pp. 752–761, 2023.
21. Y. Li and S. Tong, “Adaptive backstepping control for uncertain nonlinear strict-feedback systems with full state triggering,” Automatica, vol. 163, p. 111574, 2024.
22. X. Jin, S. Wang, J. Qin, W. X. Zheng, Y. Kang, “Adaptive fault-tolerant consensus for a class of uncertain nonlinear second-order multi-agent systems with circuit implementation,” IEEE Transactions on Circuits and Systems-I: Regular Papers, vol. 65, no. 7, pp. 2243-2255, 2018.
23. Z. Liu, H. Gao, X. Yu et al., “B-spline wavelet neural-network-based adaptive control for linear-motor-driven systems via a novel gradient descent algorithm,” IEEE Transactions on Industrial Electronics, vol. 71, no. 2, pp. 1896–1905, 2024.
24. C. Deng, X.-Z. Jin, W.-W. Che, H. Wang, “Learning-based distributed resilient fault-tolerant control method for heterogeneous MASs under unknown leader dynamic,” IEEE Transactions on Neural Networks and Learning Systems, vol. 33, no. 10, pp. 5504-5513, 2022.
25. Y. Hou, X. Jin, “Robust adaptive formation compensation control of coupled Euler-Lagrange systems, Journal of Control and Decision,” DOI: 10.1080/23307706.2025.2608802
26. A. Naderolasli, K. Shojaei, and A. Chatraei, “Finite-time velocity-free adaptive neural constrained cooperative control of Euler–Lagrange systems,” Transactions of the Institute of Measurement and Control, vol. 47, no. 12, pp. 2524–2539, 2025.
27. Z.-Y. Zhao, X.-Z. Jin, X.-M. Wu, H. Wang, J. Chi, “Neural network-based fixed-time sliding mode control for a class of nonlinear Euler-Lagrange systems,” Applied Mathematics and Computation, vol. 415, p. 126718, 2022.
28. S. Dong, K. Liu, M. Liu et al., “Adaptive neural network-quantized tracking control of uncertain unmanned surface vehicles with output constraints,” IEEE Transactions on Intelligent Vehicles, vol. 9, no. 2, pp. 3293–3304, 2024.
29. H. Feng, Q. Song, S. Ma et al., “A new adaptive sliding mode controller based on the RBF neural network for an electro-hydraulic servo system,” ISA Transactions, vol. 129, pp. 472–484, 2022.
30. G. Lu, Z. Peng, H. Wang, L. Liu, D. Wang, and T. Li, “Extended-state-observerbased distributed model predictive formation control of under-actuated unmanned surface vehicles with collision avoidance,” Ocean Engineering, vol. 238, p. 109587, 2021.